REGULAR PAPER

F. J. Huera-Huarte · P. W. Bearman

DPIV in the wake of a tandem arrangement of two flexible circular cylinders

Abstract Visualization of the wake of a system of two circular cylinders in tandem is presented through Digital Particle Image Velocimetry results in a plane perpendicular to the models' axes. Both cylinder models have an aspect ratio (length over diameter) of almost 100, a mass ratio (mass divided by mass of displaced fluid) under 2, and they are flexible and free to move in the in-line and cross-flow directions. A supporting structure provided attachment of both models through universal joints at each end and the cylinders were exposed to a uniform flow profile over the lower 45% of their lengths, producing vortex-induced vibrations with wake interactions. The centre to centre separation between the models could be varied and data is shown here for three separations of 2, 3 and 4 diameters.

1 Introduction

Groups and bundles of cylindrical components are common in offshore structures, heat exchangers and power transmission lines. The vibrations induced by vortex shedding and by interaction of the wakes of pairs of cylindrical bodies in tandem arrangements have been studied in the past as an idealisation of the very complex flow-induced vibration problems often found in practical engineering systems.

Bokaian and Geoola (1984) carried out experiments with a fixed circular cylinder placed in front of a second one which consisted of a length of rigid cylinder which was flexibly mounted. We refer to this second cylinder as being a 'rigid model'. They observed both vortex-induced vibrations (VIV) and wake-induced vibration (WIV) which they described as galloping. Zdravkovich (1985) studied different set ups of staggered, side-by-side and tandem arrangements of flexible cantilevers in a wind tunnel. His models had an aspect ratio 10 times smaller than the one presented here and a considerably high mass ratio (mass divided by mass of displaced fluid). In the tandem arrangement for a separation of 2.5 diameters centre to centre, he found a bi-stable regime which was related to the onset of regular vortex shedding from the upstream body. For gap distances in the range from 2.5 to 4 diameters he found that the response was larger for the upstream body. Mahir and Rockwell (1996) conducted experiments with two circular cylinders in forced vibration at gap distances of 2.5 and 5 diameters. They showed the different attainable lock-in states of the system in the form of Arnold tongues for each separation. They also performed flow visualisation of the wake of the system by means of the hydrogen bubble technique. Laneville and Brika (1999) studied two different

F. J. Huera-Huarte (✉)
Graduate Aerospace Laboratories, California Institute of Technology, Pasadena, CA 91125, USA
E-mail: fhuera@caltech.edu; francisco.huera@urv.cat

P. W. Bearman
Department of Aeronautics, Imperial College London, London SW7 2AZ, UK

situations, in the first a flexible cylinder was located in the wake of a stationary one and in the second the upstream cylinder was also allowed to freely vibrate. The experiments were carried out in a wind tunnel with large gap distances in the range from 7 to 25 diameters. Hover and Triantafyllou (2001), Xu et al. (2003) and Assi et al. (2006) carried out experiments with stationary leading cylinders and downstream ones which were free to vibrate in the transverse direction. Both reported a galloping-like response of the rear cylinder with large amplitudes. Flow visualisation or digital PIV (DPIV) investigations of the wakes of tandem arrangements of rigid, flexibly mounted circular cylinders are not common in the literature and to the knowledge of the authors, there are no publications showing the wakes of a pair of cylinders when both are flexible, as in the present study. In the work described here planar DPIV results are shown for separation distances (S) of 3 and 4 diameters centre to centre. Distances less than these are uncommon in offshore structures as smaller separations could result in clashing between the different structural elements (Huera-Huarte and Bearman 2008).

2 Experimental set-up

The experiments were carried out in a free surface water tunnel with a test section 0.6×0.75 m and a length of 8 m. The set up was based on that used in previous experiments with a single cylinder model and a detailed description of the experimental arrangement appears in Huera-Huarte and Bearman (2009a, b). The models were 1.5m long and had an external diameter (D) of 16 mm, giving an aspect ratio $L/D = 94$. They were mounted such that their line of centres was in the flow direction. Both models were attached to a supporting structure with universal joints at each end. During each of the experiments the two models were partially submerged in the tank and exposed to a uniform current in the lower 45% of their lengths, as seen in Fig. 1. The supporting structure allowed changes in the gap distance between the models and changes to the top tension applied to the models which resulted in changes in their natural frequencies. The dynamic response of the tandem cylinders was also studied and was briefly reported by Huera-Huarte and Bearman (2008), where the motion of the models was measured and the relationship between them was studied.

The DPIV data presented here was obtained using Digital Particle Velocimetry (DPIV). As indicated in Fig. 1, a planar horizontal laser sheet, perpendicular to the axes of the cylinders, was used to illuminate the seeding particles in the water. A digital video camera recorded the pulsed laser illuminated images by means of a CCD sensor with $1,600 \times 1,186$ pixels, a resolution of almost 2 Mpixel and a pixel size of 7.4 μm. The distance from the image plane to the sensor plane and the focal length of the camera lens combined, provided a magnification of 1/28.08. The time Δt between laser pulses was 0.0015 s and the sampling
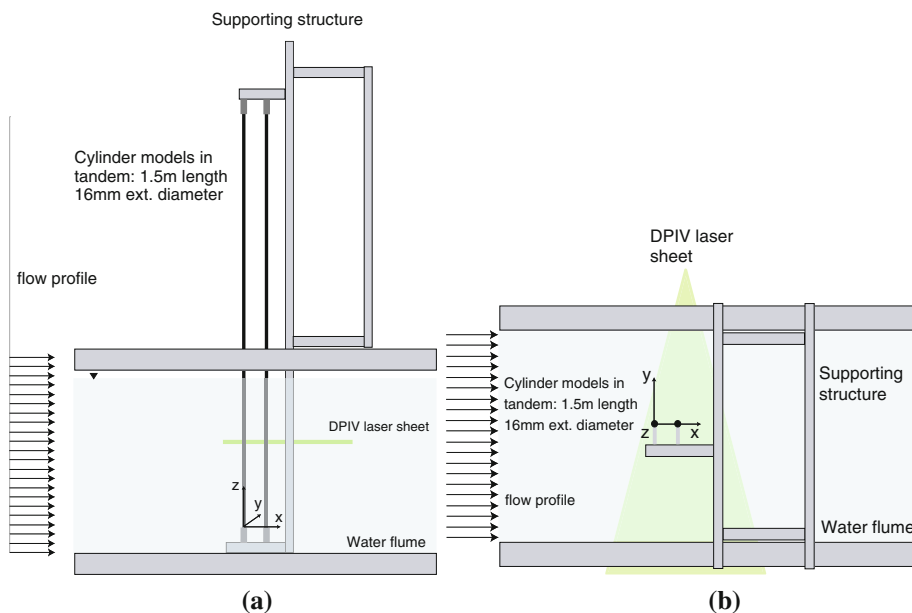

Fig. 1 Experimental set up. **a** Side view, **b** top view

frequency used was the maximum permitted by the system, 15 Hz. Hence, after the image processing which involved several steps, velocity fields in the wakes of the cylinders were obtained every 1/15th of a second. Briefly, the processing consisted of an initial step in which parts that were unavoidable, such as the supporting structure in the lower end of the field of view, were masked as they did not contain seeding particles. A cross-correlation algorithm (Willert and Gharib 1991) was applied to the masked images, based on an interrogation area of 32×32 pixels with 50% of overlapping. Outlier vectors outputted by the cross-correlation scheme were identified after comparison with neighbouring vectors and replaced by new values obtained from averaging an area of 5×5 vectors around the outlier. The last step before the calculation of the vorticity was the application of a moving average filter with the objective of removing noise which can be especially problematic when calculating derivative quantities such as vorticity.

In regions of the flow field where no strong gradients exist and the flow is expected to be uniform, the raw vectors should be very alike and also very similar to the processed vectors (validated for outliers and filtered). The uncertainty in the velocity measurements can be estimated from the temporal and spatial fluctuation of the velocity field, and it provides an indication of the error expected in the results. A final value for the error is very difficult to obtain as it depends on the resolution, the seeding density, the instantaneous velocity gradients and the turbulence intensity of the facility among others. For the cases presented here, the velocity scatter obtained from a region well away from the cylinders where the flow is expected to be uniform, was found to be around 0.042 pixels, which corresponds to a velocity of around 0.6 cm/s. A discussion on sources of error associated to DPIV appears in Willert and Gharib (1991) and in more detail regarding the processing techniques in Huang et al. (1997). Here, the main objective was the study of the flow topology in terms of the identification of large vortical structures being shed from the cylinders and the existence or not of a separated wake between the two cylinders with or without reattachment of the shear layers. Vorticity appears in all figures based on the same scale in all snapshots for easy comparison, and it has been non-dimensionalised using the free stream velocity and the cylinder diameter.

3 Results

A total of four DPIV runs are presented in this paper. Two (cases 1 and 2) are for a centre to centre separation of 3 diameters and the other two (cases 3 and 4) for a separation of 4 diameters. To provide suitable comparisons, at each separation one of the runs shows the results when there is practically no motion of the cylinders (cases 1 and 3), and the other shows results for large motions of both cylinders (cases 2 and 4). In cases 1 and 3, the flow speed (V) was 0.25 m/s and the top tension (T_t) applied to the models was 110 N. The resulting Reynolds number (Re) was around 3,500 and the reduced velocity ($V_1 = \frac{V}{f_1 D}$) based on the fundamental natural frequency of the downstream cylinder in still water (f_1), was about 2.1. In cases 2 and 4, the top tension was the same but the flow speed was 0.6 m/s resulting in a Re of 8,400 and a V_1 of 5. For each of these four cases the dynamic response is also presented. The dynamic response of another experiment with a gap separation of 2 diameters (case 5) is also shown. In case 5, the flow speed was 0.5 m/s and the top tension was 60 N resulting in $V_1 = 5.7$, $Re = 7,000$. Cases 2, 4 and 5 are good examples of periodic large motions in both cylinders for V_1 inside the range from 5 to 6, where the measured amplitudes were a maximum for all separations.

Figures 2, 3, 4, and 5 show vorticity fields with clockwise vorticity in blue and counter clockwise vorticity in red. These plots provide visualisation of vortex formation and the evolution of the wakes of the cylinders. In all the plots the cylinder cross sections, at the height at which the interrogations were performed, are shown with solid gray circles. The flow goes from top to bottom and each realisation is separated by 2/15th of a second, starting from the left plot (a). The region shown in each image covers an area of 7×11 diameters. The origin of the coordinate system is coincident with the axis of the upstream cylinder in its initial configuration at rest. Three vertical dashed lines located at $y/D = -1$, 0 and 1 are used in each figure to allow an easy identification of the instantaneous positions of the cylinders in the interrogation area. Horizontal lines for the same purpose are located at $x/D = 0$, 5 and 10 from the top of each image.

Assuming Strouhal numbers around 0.17, as suggested in previous experiments with a flexible cylinder at similar Reynolds numbers (Huera-Huarte and Bearman 2009a), the vortex shedding frequency (f_s) for cases 1 and 3, with flow speeds of 0.25 m/s, would be around 2.6 Hz and for cases 2 and 4, with speeds of 0.6 m/s, it would be near 6.4 Hz. The lack of motion of the cylinders in cases 1 and 3 is due to the fact that f_s was significantly lower than f_1, which was over 7 Hz for the tension used in cases 1–4 (Huera-Huarte and Bearman 2009a). For cases 2 and 4, the excitation frequency f_s was relatively close to f_1 and hence excitation
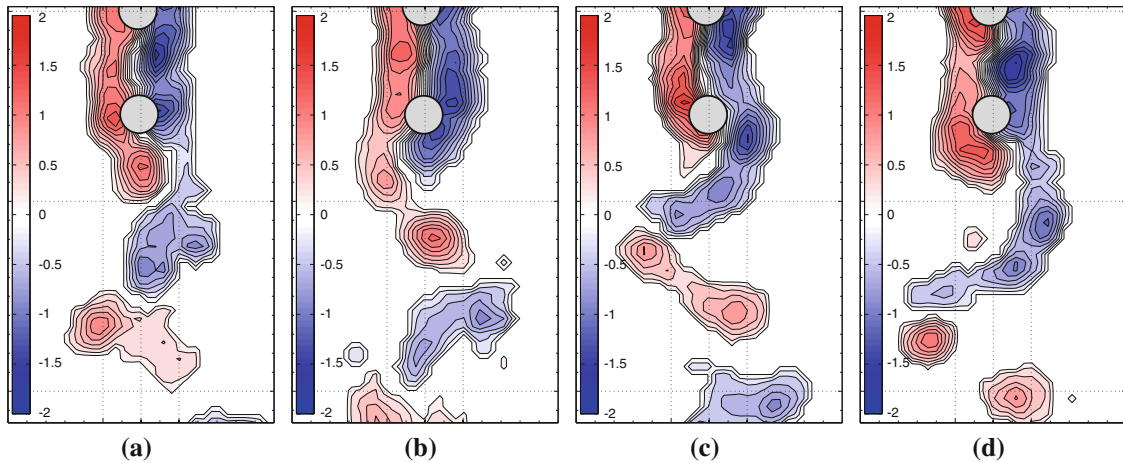
Fig. 2 Case 1: Centre to centre separation $S/D = 3$, $V = 0.25$ m/s, $T_t = 110$ N, $Re = 3500$, $V_1 = 2.1$
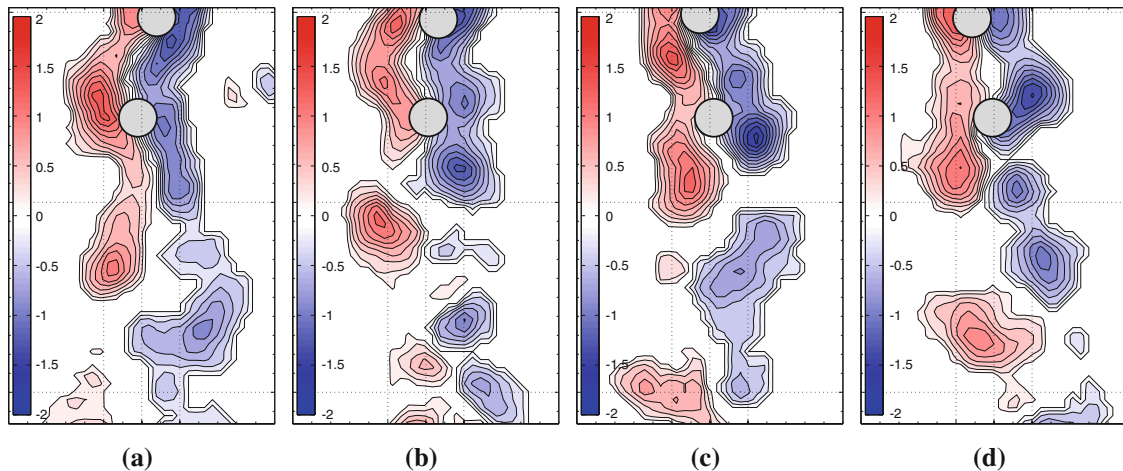

Fig. 3 Case 2: Centre to centre separation $S/D = 3$, $V = 0.6$ m/s, $T_t = 110$ N, $Re = 8400$, $V_1 = 5$

was observed. Figure 2 for case 1 shows that there is no shedding ahead of the trailing cylinder but a region of separated flow that reattaches to the downstream body, generating the shedding of well defined alternating vortices behind the trailing cylinder. In Fig. 4 for case 3, the downstream cylinder is not near enough to the upstream body to suppress the shedding between the models and hence the vortices that are being shed from the front cylinder, impinge on the rear cylinder and combine with vortices from the rear cylinder. The upcoming vortices from the front cylinder were not able in this case to excite the downstream cylinder. In experiments by Zdravkovich (1985) two regimes were distinguished, one in which the shedding from the front cylinder was suppressed and another in which shedding existed separately for both cylinders. In the regime with suppressed shedding between the cylinders, the leading body showed considerably larger amplitudes than the trailing one. The values presented in Table 1, the DPIV plots in Figs. 3 and 5 for cases 2 and 4, and the dynamic response plots in Fig. 6 confirm that finding. The motion of the upstream cylinder for gap separations of 2, 3 and 4 diameters, where either there is no wake between the cylinders or there is a wake with intermittent reattachment, is larger than the motion of the downstream one. Evidence of these larger motions in the upstream cylinder for S/D in the range from 1.5 to 4 were also provided in Huera-Huarte and Bearman (2008).

In Fig. 6a–c the dynamic response of the cylinders is shown for cases 5, 2, and 4, respectively. These are results obtained from strain gauges installed in the cylinders and from laser displacement sensor measurements (Huera-Huarte and Bearman 2008). The same instrumentation was also used in single cylinder experiments, and further details can be seen in Huera-Huarte and Bearman (2009a). For each case the time
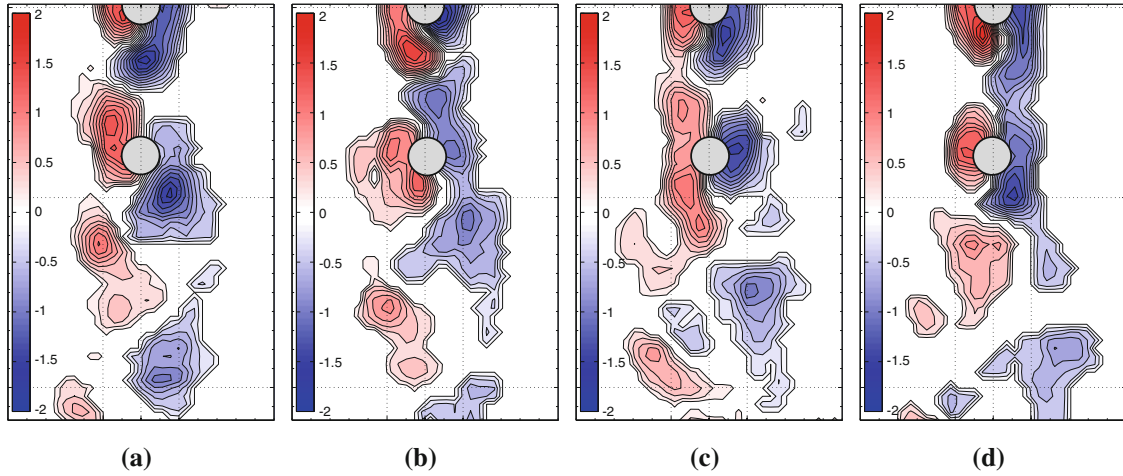
Fig. 4 Case 3: Centre to centre separation $S/D = 4$, $V = 0.25$ m/s, $T_t = 110$ N, $Re = 3500$, $V_1 = 2.1$

Table 1 Summary of amplitudes and phase differences for cases 2, 4 and 5

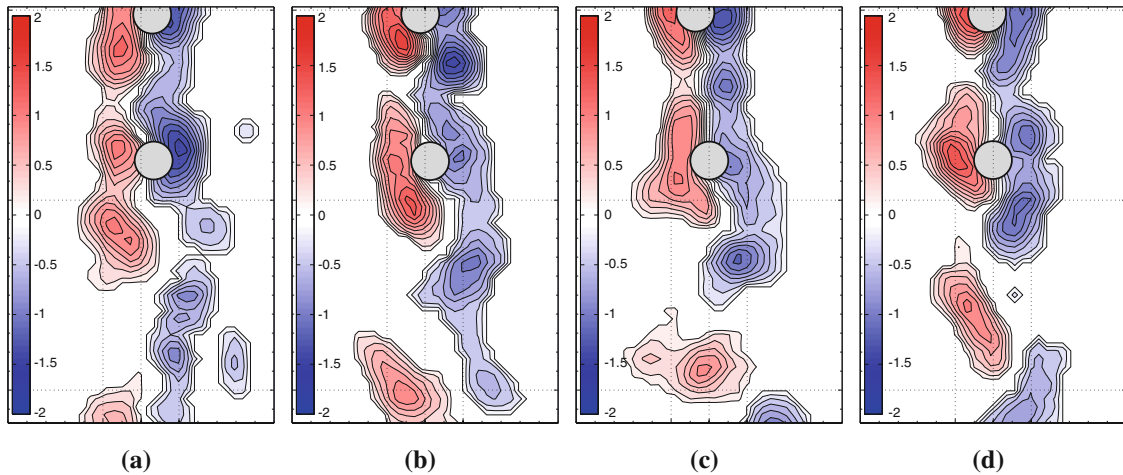|	Case 5($S/D = 2$)			Case 2($S/D = 3$)			Case 4($S/D = 4$)			Case SINGLE	
	UC	DC	%	UC	DC	%	UC	DC	%		%
y_M/D	1.06	0.42	60	0.92	0.83	10	0.9	0.73	19	0.68	25
y_{RMS}/D	0.73	0.21	71	0.58	0.52	10	0.55	0.48	13	0.28	49
y_H/D	1.03	0.29	62	0.82	0.73	11	0.78	0.68	13	0.58	26
Φ (deg)		4			27			-30			

Fig. 5 Case 4: Centre to centre separation $S/D = 4$, $V = 0.6$ m/s, $T_t = 110$ N, $Re = 8400$, $V_1 = 5$

series of the transverse displacement at the mid point of the models is provided in the first column on the left, in red for the upstream cylinder and in blue for the downstream one. In that column the envelope of the motions, obtained by means of the Hilbert transform, appears in black. Also a dashed line indicating the root mean square (RMS) value of the signal is provided. The second column shows the spectra of each signal with very clear peaks in all of them indicating strong periodicity. The last column depicts an enlargement of a second inside the run and also a plot where both signals appear plotted against each other. These two last plots provide an intuitive way of calculating the phase difference between the transverse motions of the cylinders. Table 1 gives the representative values for each one of these test conditions plus the values resulting from a test with a single cylinder reported Huera-Huarte and Bearman (2009a) having the same parameters (applied tension and flow speed and hence same V_1 and Re), in the last column. The first row
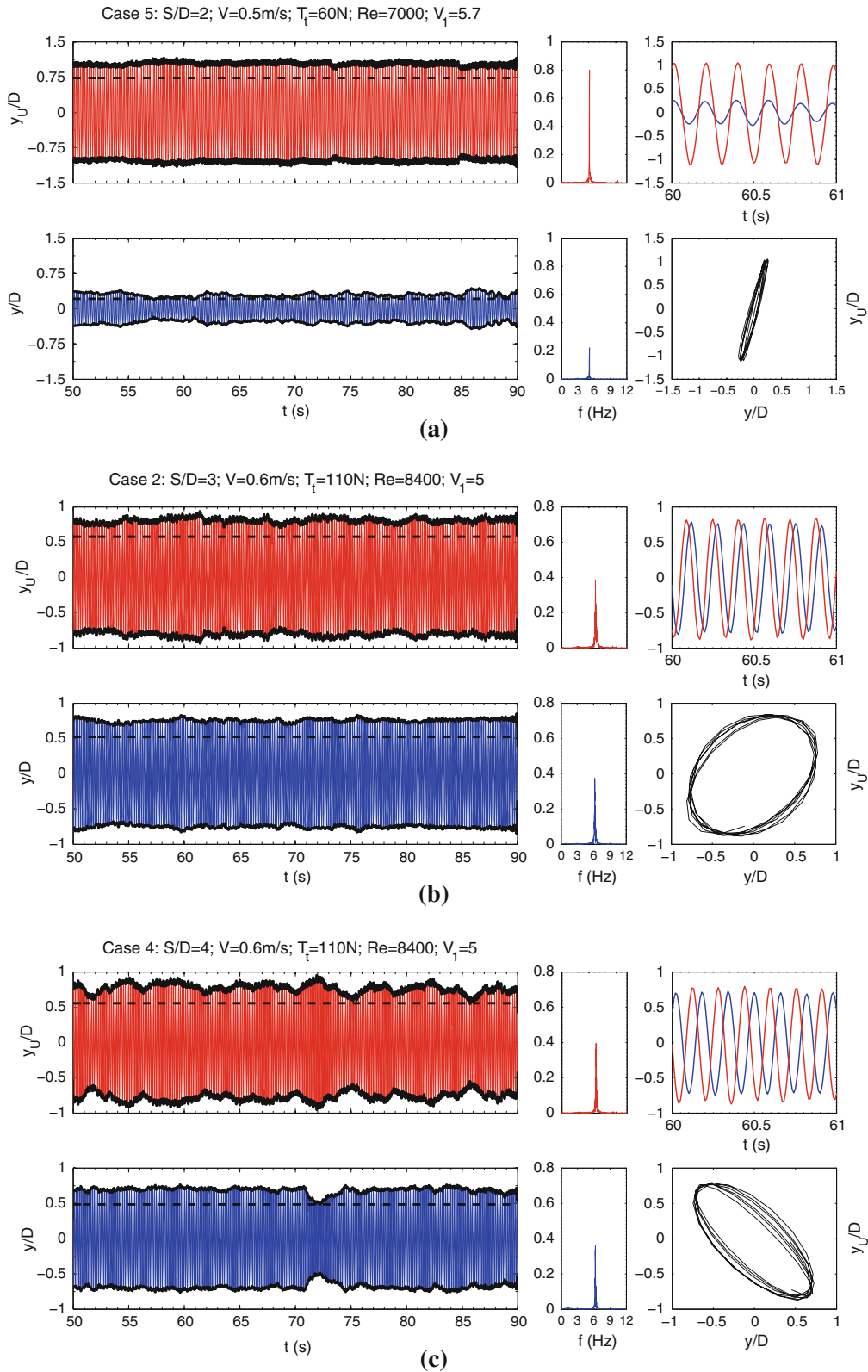
Fig. 6 Transverse amplitudes (*column one*) and spectra (*column two*) of the cylinders for cases 2 (**b**), 4 (**c**) and 5 (**a**). *Red* accounts for the upstream cylinder (y_U/D) and *blue* for the downstream one (y/D). Envelopes (calculated with Hilbert transforms) appear in black. The horizontal *black dashed line* is the RMS of the signals. The *third column* shows and enlargement showing the 60th second of both signals and a plot to see the phase difference between both signals

gives the maximum amplitude (y_M/D), the second the RMS (y_{RMS}/D), the third is the mean of the envelope (y_H/D) and the last the phase difference (Φ). The differences in the amplitudes are given as a percentage of the upstream amplitudes. UC and DC are used for upstream and downstream cylinders, respectively. One has to bear in mind that the DPIV interrogations were made well bellow the mid points of the models and that is why the amplitudes that appear in Figs. 3 and 5 are less than 50% of those in Fig. 6 and Table 1. The figures and the table show how the transverse motion of the UC is always larger than the DC one. For gap separations of 3 or 4 diameters, the differences are somewhere between 10 and 20% but in the case of 2 diameters of separation, the difference is strikingly around 65%, depending on which value you look at. In the last column of the table, one can see that the relative difference between the amplitudes of the single cylinder case and Case 4 go from 25 to 49% depending what value we consider.

In case 2, large transverse oscillations of the front cylinder are triggered and govern the interaction. The shear layers separating from the upstream cylinder reattach to the rear cylinder producing a common wake which is formed from the upstream body and disrupts the formation from the rear cylinder, reducing its motion. Even though DPIV is not available for case 5 with the smallest gap distance, the data in Fig. 6a suggests that the common wake effect is especially strong, producing a very large difference in the transverse amplitudes of the cylinders. If the separation is increased to 4D in Fig. 5 for case 4, alternating vortex shedding appears between the cylinders with intermittent reattachment. The amplitudes of the upstream body are not as regular and vigorous as in cases 2 and 5, the maximum values are very similar to those in case 2 but the mean of the envelopes and the RMS are smaller. As the gap between the cylinders increases, amplitudes are expected to become more like those found for a single cylinder as the interaction between the wakes weakens because of the larger gap.

This fluid–structure interaction mechanism is very different to that reported by other authors. In the case of two tandem rigid cylinder models, if the upstream body is fixed and the rear one is free to vibrate, the fluid elastic excitation results in WIV with galloping-like larger responses for the rear body. This phenomenon occurs at reduced velocities above those for VIV (Bokaian and Geoola 1984; Zdravkovich 1985; Assi et al. 2006). In the experimental arrangement presented here, with both cylinders flexible and free to move, as the reduced velocity is increased and the vortex shedding frequency passes through the regime for expected VIV, the amplitudes are larger for the leading cylinder.

4 Conclusions

Vorticity fields obtained by using Digital Particle Image Velocimetry in the wakes of two flexible oscillating cylinders in a tandem arrangement have been presented in this paper. Most of the previous studies were based on fixed cylinders or flexibly mounted rigid cylinders. High aspect ratio cylinder experiments are difficult to design and even more difficult if visualization of the wake is attempted. To the knowledge of the authors, no DPIV data has been previously reported for wake visualization of two freely vibrating pin-jointed flexible cylinders in tandem.

The upstream cylinder in tandem arrangements, with gap distances of 4 diameters or smaller, undergoes larger transverse vibrations than the rear one when both are free to move. These vibrations can be over one diameter, larger (at least more than 25%) than those observed with the same set-up in a single cylinder experiment (Huera-Huarte and Bearman 2009a). The differences in the transverse amplitude attained by the front cylinder are a function of the gap distances and in general the closer the models are, the larger the motion of the upstream body. This is closely related to the existence or not, of alternating vortex shedding between the cylinders or a reattachment of the shear layers to the rear body. As the separation between the cylinders is increased the coupling through the wake reattachment becomes weaker and they start to respond more like what might be expected of single cylinders.

References

Assi GRS, Meneghini JR, Aranha JAP, Bearman PW, Casaprima E (2006) Experimental investigation of flow-induced vibration interference between two circular cylinders. J Fluid Struct 22:819–827
Bokaian A, Geoola F (1984) Wake-induced galloping of two interfering circular cylinders. J Fluid Mech 146:383–415

Hover FS, Triantafyllou MS (2001) Galloping response of a cylinder with upstream wake interference. J Fluid Struct 1:503–512

Huang H, Dabiri D, Gharib M (1997) On errors of digital particle image velocimetry. Meas Sci Technol 8:1427–1440

Huera-Huarte FJ, Bearman PW (2008) Wake structures and dynamic response of one and two long flexible cylinders undergoing vortex-induced vibrations. In: Proceedings of the 9th international conference on flow-induced vibrations, Prague

Huera-Huarte FJ, Bearman PW (2009a) Wake structures and vortex-induced vibrations of a long flexible cylinder—part 1: dynamic response. J Fluid Struct 25:969–990

Huera-Huarte FJ, Bearman PW (2009b) Wake structures and vortex-induced vibrations of a long flexible cylinder—part 2: drag coefficients and vortex modes. J Fluid Struct 25:991–1006

Laneville A, Brika D (1999) The fluid and mechanical coupling between two circular cylinders in tandem arrangement. J Fluid Struct 13:967–986

Mahir N, Rockwell D (1996) Vortex formation from a forced system of two cylinders—part i: tandem arrangement. J Fluid Struct 10:473–489

Willert C, Gharib M (1991) Digital particle image velocimetry. Exp Fluids 10:181–193

Xu SJ, Zhou Y, Mi J (2003) Flow visualization behind a streamwise oscillating cylinder and a stationary cylinder in tandem arrangement. J Vis Japan 7-3:201–208

Zdravkovich MM (1985) Flow induced oscillations of two interfering circular cylinders. J Sound Vib 101:511–521